# Magnetic properties of bridged azido complexes

*Yu. V. Rakitin* and V. T. Kalinnikov*

*I. V. Tananaev Institute of Chemistry and Technology of Rare Elements and Mineral Raw Materials, Kola Scientific Center of the Russian Academy of Sciences, 26a ul. Fersmana, 184209 Apatity, Russian Federation. Fax: +7 (815 55) 79414. E-mail: office@chemy.kolasc.net.ru*

It was shown on the basis of the generalized angular overlap model that specific features of the electronic structure of the $N_3^-$ anion in polynuclear complexes with the $M(\mu_{1,1}\text{-}N_3)_2M$ magnetic fragment should result in strong ferromagnetism. The $\mu_{1,3}\text{-}N_3$ coordination mode favors antiferromagnetic properties. The theoretical results agree with experimental magneto-structural correlations.

**Key words:** transition metals, azido complexes, ferromagnetism, antiferromagnetism.

Polynuclear complexes of transition metals with the $N_3^-$ bridging ligands manifest such a wide variety of properties from strong antiferromagnetism to strong ferromagnetism that $N_3^-$ was named an ideal ligand for design of molecular magnetics.[1] In this work, we analyzed the influence of specific features of the electronic structure of this linear ligand on the magnetic properties of complexes in the framework of the modern theory of exchange interactions and the generalized angular overlap model.[2—4] The development of this theory is urgent, because the popular model of spin polarization of the $N_3^-$ ligands proposed[5] to explain ferromagnetism of the $L_nM(\mu_{1,1}\text{-}N_3)_2ML_n$ complexes has not been confirmed by a recent neutron diffraction study.[6] Below we shall show that the theoretical results agree well with experimental data.

## Theory

The modern theory of magnetic exchange interactions is based on the Hay—Thibeault—Hoffman model,[7] according to which the exchange parameter $-2J$ for homodinuclear systems is the following:

$$-2J = -2J^{f} - 2J^{af} = \Sigma_{ij} - 2J_{ij}/(4S_aS_b) = \\ = [\Sigma_{ij} - 2J_{ij}^{f} + \Sigma_i\Delta^2(ia,ib)/K_{ab}]/(4S_aS_b). \quad (1)$$

Here $S_a$ and $S_b$ are spins of the metal ions a and b, respectively, and indices $i$ and $j$ numerate orbitals of unpaired electrons of these ions. In the antiferromagnetic contribution $-2J^{af}$, the magnitude $K_{ab} = 5—10$ eV [7] has a sense of the metal—metal charge transfer energy and is rather stable for atoms of the same transition series.[2] The $\Delta(ia,ib)$ parameters are the differences between the energies of MO $|\psi\pm\rangle$ of the dimer or dimeric fragment, which are formed by orbitals of unpaired electrons of mononuclear fragments $|ia\rangle$ and $|ib\rangle$: $|\Delta(ia,ib)| = |E(\psi+) - E(\psi-)|$. These MO should be related by a symmetry operation, so that $|\psi\pm\rangle \sim(|ia\rangle\pm|ib\rangle)$. In the case of heterodinuclear systems, the estimates of $-2J^{af}$ somewhat increase but remain low for metals of the same Period.[8]

Rewrite expression (1) in the form

$$-2J_\Sigma = \Sigma_{ij} - 2J_{ij} = -2J\cdot 4S_aS_b. \quad (2)$$

Unlike $-2J$, the $-2J_\Sigma$ value is independent of the spin factor and is determined only by contributions of pairwise interacting orbitals. Therefore, this magnitude has a physical sense of the exchange energy and can conveniently be used for analysis of changes in mechanisms of exchange interactions when paramagnetic ions with different numbers of unpaired electrons are replaced.

The determination of the $|\psi\pm\rangle$ orbitals and $\Delta(ia,ib)$ splittings for the triatomic linear fragment is shown in Fig. 1. It is seen that the antiferromagnetic contribution has the same nature as the chemical bond and, hence, the

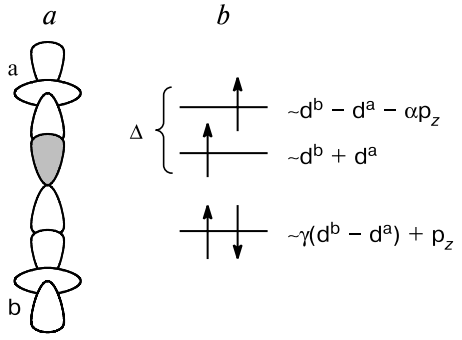


**Fig. 1.** Antiferromagnetic interaction of unpaired electrons of two centers through the occupied orbital of the ligand (*a*) and the corresponding scheme of molecular orbitals (*b*).

Published in Russian in *Izvestiya Akademii Nauk. Seriya Khimicheskaya,* No. 4, pp. 731—739, April, 2004.

1066-5285/04/5304-0766 

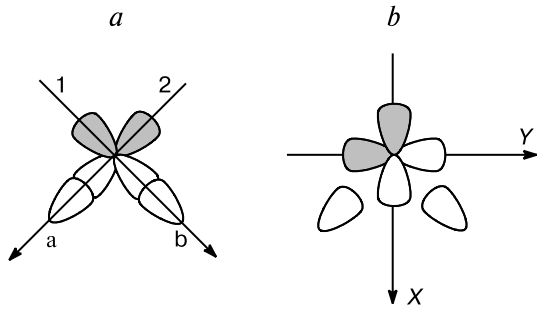


**Fig. 2.** Ferromagnetic interaction of unpaired electrons of two centers through the orthogonal orbitals of the ligand (*a*) and the equivalent scheme of the same triatomic fragment (*b*).

presence of an effective metal—ligand—metal (MLM) overlap chain always produces strong antiferromagnetism.[9]

The predominant part of the $-2J_{ij}^{f}$ ferromagnetic contributions is expressed through combinations of one-center integrals of the bridging ligand.[2] Therefore, they are proportional to the product of squared amplitudes of unpaired electrons directed to the ligand.

The $-2J_{ij}^{f}$ values change slightly with a change in the M—L—M angle. On the contrary, the antiferromagnetic contributions depend strongly on this angle. For instance, the scheme of 90° exchange is presented in Fig. 2, *a*. It can be seen that, unlike the 180° exchange (see Fig. 1), the antiferromagnetic contribution for the 90° exchange is zero, because the orbitals of two centers are orthogonal and $\Delta(i\mathrm{a},i\mathrm{b}) = 0$. Therefore, only the ferromagnetic contribution remains for the 90° exchange. The equivalent scheme corresponding to the unitary basis transform $p_{x,y} = (p_1 \pm p_2)/\sqrt{2}$ is shown in Fig. 2, *b*. If the M—L—M angle is 90°, then $E(|\psi+\rangle \sim |a\rangle + \alpha p_x + |b\rangle) = E(|\psi-\rangle \sim |a\rangle + \alpha p_y - |b\rangle)$, and the antiferromagnetic contribution vanishes.

Thus, the study of regular changes in the $-2J$ value in series of related compounds is reduced, first of all, to analysis of the antiferromagnetic contribution. However, according to Eq. (1), the $-2J^{af}$ value depends, in turn, on the difference of the MO $|\psi\pm\rangle$ energies, which makes it possible to use the theoretical tools of the MO method for this analysis. In particular, the generalized angular overlap model (AOM)[3,4] is very convenient for calculation of the $\Delta(i\mathrm{a},i\mathrm{b})$ values.

According to this model, the matrix elements of the effective Hamiltonian for metal orbitals $(i, j)$ are the sum over all orbitals of ligands $(m, n)$, which overlap the $(i, j)$ orbitals

$$h_{ij} = \sum_{mn} (H_{\mathrm{ML}} - H_{\mathrm{d}}S_{\mathrm{ML}})_{im} (H_{\mathrm{d}}S_{\mathrm{LL}} - \mathrm{H}_{\mathrm{LL}})_{mn}^{-1} \cdot (H_{\mathrm{LM}} - H_{\mathrm{d}}S_{\mathrm{LM}})_{nj}. \quad (3)$$

Here the $H_{\alpha\beta}$ and $S_{\alpha\beta}$ symbols designate the blocks of matrices of the Hamiltonian and overlap integrals. When developing the parametric theory, it is enough to approximate the matrix elements $H_{\alpha\beta} = \langle\alpha|H|\beta\rangle$ according to Mulliken—Wolfsberg—Helmholz[10,11]:

$$H_{\alpha\alpha} = H_{\alpha}, H_{\alpha\beta} \approx (H_{\alpha} + H_{\beta})S_{\alpha\beta}. \quad (4)$$

In the case of pairs of orbitals we are interested in ($i$a and $i$b), Eq. (3) is reduced to

$$\begin{matrix} \langle i\mathrm{a}| \\ \langle i\mathrm{b}| \end{matrix} \begin{bmatrix} h_{i\mathrm{a},i\mathrm{a}} & h_{i\mathrm{a},i\mathrm{b}} \\ h_{i\mathrm{a},i\mathrm{b}} & h_{i\mathrm{b},i\mathrm{b}} \end{bmatrix}. \quad (5)$$

Since for symmetry of the problem $h_{i\mathrm{a},i\mathrm{a}} = h_{i\mathrm{b},i\mathrm{b}}$, then

$$\Delta(i\mathrm{a},i\mathrm{b}) = 2h_{i\mathrm{a},i\mathrm{b}}. \quad (6)$$

It follows from this and Eq. (3) that for monoatomic ligands

$$\Delta(i\mathrm{a},i\mathrm{b}) = 2\Sigma\lambda e_{\lambda}\langle i\mathrm{a}|\lambda\rangle\langle\lambda|i\mathrm{b}\rangle, \quad (7)$$

where the index $\lambda = \sigma, \pi, \ldots$ numerates the orbitals of the ligands and the type of their overlap with the orbitals of the metal atoms, and $e_{\lambda}$ has a sense of the antibonding energy of the metal—ligand diatomic bond of the $\lambda$ type.[3,4] The $\langle i|j\rangle$ symbols designate the angular parts of the overlap integrals. For elements of the first transition series and electronegative ligands, $e_{\sigma} = (4\text{—}6) \cdot 10^3$ cm$^{-1}$ and $e_{\pi} \sim 10^3$ cm$^{-1}$.[4] In the case of strong $\sigma$-interactions, $\pi$-overlaps can be neglected, because $-2J^{af} \sim \Sigma\Delta^2$.

Returning to Fig. 2, *b* and inserting the overlap integrals $\langle\mathrm{a},\mathrm{b}|\mathrm{p}_x\rangle = \cos(\theta/2)$ and $\langle\mathrm{a},\mathrm{b}|\mathrm{p}_y\rangle = \pm\sin(\theta/2)$, where $\theta$ is the M—L—M angle, into Eq. (7), we find

$$\Delta(i\mathrm{a},i\mathrm{b}) = 2h_{i\mathrm{a},i\mathrm{b}} = 2e_{\sigma}[\cos^2(\theta/2) - \sin^2(\theta/2)] = 2e_{\sigma}\cos\theta. \quad (8)$$

This formula agrees completely with Fig. 2 and predicts that $-2J^{af} \sim \Delta^2(i\mathrm{a},i\mathrm{b}) = 0$, if $\theta = 90°$. Sometimes a weak interaction of the metal orbitals with the low-lying s-orbital of the ligand is also taken into account. This leads to the appearance of an angle-independent term in Eq. (7), and Eq. (8) is modified to the form

$$\Delta(i\mathrm{a},i\mathrm{b}) = 2e_{\sigma}(\cos\theta + s^2). \quad (9)$$

Formula (9) predicts that $\Delta(i\mathrm{a},i\mathrm{b}) = 0$ for $\theta_0 \geq 90°$. This conclusion agrees well with the modern theoretical concepts[2,4] and experimental data. In particular, for NiO $s^2 \approx 0.2$,[2] which corresponds to $\theta_0 \approx 102°$.

### Electronic structures of the $N_3^-$ linear anions

For calculations by formula (3), it is not difficult to go from monoatomic to polyatomic ligands, because no diagonalization is needed and only the Hamiltonian submatrix for ligands should be inverted. Unlike diagonalization, inversion can also be made in the analytical form. However, for the $N_3^-$ ligands, these transformations give

complicated expressions, which do not allow one to reveal the physical sense of the effects predicted. Therefore, we used another method.

The $N_3^-$ ligand is a group of strongly bonded atoms (N—N bond length is 1.25 Å), which interact with metal atoms as a single species. Therefore, we calculated first the electronic structure of the $N_3^-$ anion and then took into account the metal—ligand interaction. Formula (3) assumes this interpretation and even becomes simplified, because the central matrix to be inverted is diagonal in the basis of eigenfunctions.

The $p_y$ and $p_z$ orbitals can be classified immediately due to a high symmetry of the ligand. In fact, it is seen from the data in Fig. 3 that the group orbital $|y-\rangle = (p_{y1} - p_{y3})/\sqrt{2}$ is non-bonding and, hence, can be involved in interaction with metal atoms. At the same time, the orbital $|y+\rangle = (p_{y1} + p_{y3})/\sqrt{2}$ forms a strong π-bond with the $p_{y2}$ orbital, so that the energies of the resulting MO differ too strongly from the energy of the d-orbitals of the metal to make the corresponding interaction efficient. The same concerns the $|z\pm\rangle$ orbitals due to the cylindrical symmetry of the ligand.

The $p_x$ orbitals interact with each other and also with the s-orbitals, so that purely symmetrical analysis is insufficient to obtain valid MO. However, the results of simple calculation by the extended Hückel method[7] show that of six resulting MO only $|x+\rangle$ and $|x-\rangle$ (see Fig. 3) have energies close to those of the d-orbitals of the metal atoms and can interact efficiently with the latter. This induces, most likely, specific features of magnetic properties of the complexes with the $N_3^-$ ligands.

When the metal atoms are arranged along the *X* axis on both sides from the ligand (coordination mode $\mu_{1,3}$), the $|x\pm\rangle$ orbitals generate antibonding of both $|\psi+\rangle$ and $|\psi-\rangle$, because $|\psi+\rangle \sim |a\rangle + \alpha|x+\rangle + |b\rangle$, and $|\psi-\rangle \sim |a\rangle + \beta|x-\rangle - |b\rangle$. The resulting compensation of contributions of the $|x\pm\rangle$ orbitals to Δ(a,b) should be rather complete, because the complex with an almost linear unit $Ni(\mu_{1,3}\text{-}N_3)Ni$ [12] is ferromagnetic. The N—N—Ni angles are usually smaller than 180°, and high antiferromagnetic

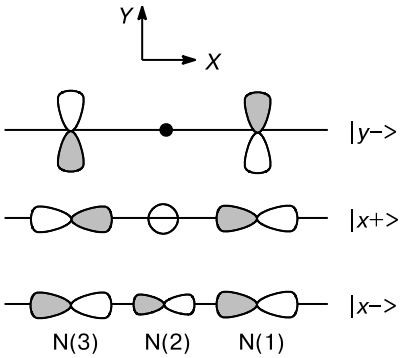


**Fig. 3.** "Magnetic" orbitals of the $N_3$ ligands; MO $|z-\rangle$ is obtained from $|y-\rangle$ by the rotation by 90° about the *x* axis.

contributions appear due to the overlap with the $|y-\rangle$ and $|z-\rangle$ orbitals (see Fig. 3).

When the metal atoms are arranged at the one side (coordination mode $\mu_{1,1}$), both $|x\pm\rangle$ orbitals contribute to the $|\psi+\rangle$ orbital, *i.e.*, behave similarly to the $p_x$ orbital in Fig. 2, *b*. Therefore, strong ferromagnetism can be expected in this case.

Let us analyze the effects considered in more detail and compare them with experimental data.

### Complexes with the $\mu_{1,3}$-$N_3$ bridging ligands

Typical structures of these complexes with one (*a*) and two (*b*) bridging ligands are presented in Fig. 4. Let us designate the N—N—M angles by symbol η, and symbol ρ will designate the angle between the corresponding planes (see Fig. 4, *c*). As mentioned in previous Section, the interaction through the $|x\pm\rangle$ orbitals is weak, and for the interaction of the σ-orbitals of two metal atoms through the $|y-,z-\rangle$ orbitals of one $\mu_{1,3}$-$N_3$ bridge, using Eqs. (3)—(6) we easily obtain

$$\Delta(a,b) \sim -\sin\eta_1 \sin\eta_2 \cos\rho. \qquad (10)$$

Here sinη are the angular parts of the overlap integrals $\langle y|\sigma\rangle$. The origin of the cosρ factor can easily be understood taking into account that the antisymmetric MO $|\psi-\rangle$ is antibonding for ρ = 0°, while for ρ = 180° the MO $|\psi+\rangle$ is antibonding (see Figs. 3 and 4, *c*), because the MO $|y-\rangle$ contain the orbitals of coordinated atoms $p_{y1}$ and $p_{y3}$ with opposite signs. Symbol "~" points to that formula (10) retains the explicit form for only angular coefficients that change from complex to complex. The other factors are grouped to form a parameter independent of angular distortions.

For example, formula (10) corresponds to the $Cu^{II}$ complexes in which the orbitals of unpaired electrons $d_{xy}$ overlap with the ligand in such a way as it is shown in Fig. 4, *c*. This structure is inherent in one of the units of the alternated chain in the $[Cu_2(tmen)_2(N_3)_2](PF_6)$ complex (tmen is *N*,*N*,*N*′*N*′-tetramethylenediamine)[13] in which $\eta_1 = 117°$, $\eta_2 = 118°$, ρ = 20°, and $-2J = 308$ cm$^{-1}$.

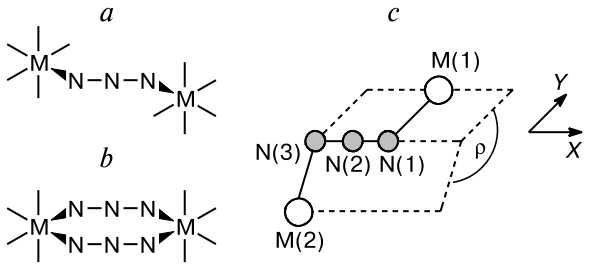


**Fig. 4.** Structures of the dinuclear fragments of the complexes with one (*a*) and two (*b*) $\mu_{1,3}$-$N_3$ bridging ligands and the scheme illustrating determination of the ρ angle (*c*).

The $[(ttz)_2Cu_2(\mu_{1,3}\text{-}N_3)(N_3)_2](ClO_4)\cdot H_2O$ dinuclear complex (ttz is *N*,*N*′*N*″-trimethyl-1,4,7-triazacyclononane)[14] in which $\eta_1 = 123°$, $\eta_2 = 121°$, $\rho = 25°$, and $-2J = 331$ cm$^{-1}$ also contains one bridge. As should be expected, both complexes are antiferromagnetic. The close exchange parameters are caused by similar structures of the magnetic fragments.

Several useful estimates can be obtained by formula (10) and parameters presented.

Since $-2J^{af} \sim \Delta^2$ and, according to Eq. (3), $\Delta$ depends linearly on the number of equivalent bridges, the duplication of the number of the latter should result in a fourfold increase in $-2J^{af}$. Therefore, it is not surprising that the complexes with the $Cu(\mu_{1,3}\text{-}N_3)_2Cu$ magnetic unit are diamagnetic[14—16]: the estimate 4(300—350) = 1200—1400 (cm$^{-1}$) corresponds to such a singlet-triplet splitting for which the magnetic triplet is not virtually populated.

Starting from expression (10) and the above-presented parameters, one can easily obtain an estimate for the maximum $-2J^{af}$ value for the exchange through one bridge corresponding to $\eta = 90°$ and $\rho = 0°$: $-2J^{af}_{max} \approx$ 600—700 cm$^{-1}$. This is a rather high value. However, this value is much lower than $-2J^{af}_{max} > 1200$ cm$^{-1}$ obtained[17] from analysis of the data for the heteroligand complex containing the $N_3$ and OR bridges. This discrepancy is caused by the underestimation[17] of a great antiferromagnetic contribution of the OR bridges. This underestimation is assumed rather frequently, despite a whole series of publications concerning this problem.[2,18,19] For instance, it follows from the $-2J(\theta)$ plot[19] that the exchange parameter increases linearly from 700 to 860 cm$^{-1}$ in the interval $\theta = 99$—$104°$. The copper(II) complexes with the monoatomic bridging ligands are usually ferromagnetic in this region of $\theta$ angles: $-2J < 0$.[2] However, the complexes, whose O—R bonds lie in the $Cu_2O$ plane, were considered.[19] According to the data,[2,18] this favors, in fact, strong antiferromagnetism.

For the $Cu^{II}$ complexes with the pronounced equatorial plane, the absence of interaction with the orbitals of unpaired electrons $|xy\rangle$ is easily monitored by an elongated metal—ligand distance. Unlike $Cu^{II}$, the $Ni^{II}$ ions usually have a slightly distorted octahedral environment, so that sometimes it is difficult to determine which of the orbitals of unpaired electrons ($|xy\rangle$ or $|z^2\rangle$) is oriented toward a given ligand. Therefore, in the two-bridge systems, both bridges can interact with the $|xy\rangle$ orbital. As a result, the $\Delta$ value doubles and $-2J^{af}$ fourfold increases compared to those in the case of one bridge. If two bridges interact with two different orbitals, then, according to Eq. (1), their contributions to $-2J^{af}$ are simply summated. It should be kept in mind that the amplitudes of the $|z^2\rangle$ and $|xy\rangle$ orbitals are in a ratio of $1 : \sqrt{3}/2$. The situation is simplest when the bridging ligands are coordinated in the equatorial plane and the $\Delta(z^2,z^2)$ contribution appears along with the $\Delta(xy,xy)$ contribution: since the amplitude of the $|z^2\rangle$ orbitals in the equatorial plane is 1/2 of the maximum amplitude and $-2J_{ij} \sim \langle M|L\rangle^4$, this contribution can be neglected. Below we will take into account these factors in selection and analysis of the experimental factors.

Let us begin from the $Ni(\mu_{1,3}\text{-}N_3)Ni$ systems. The main structural and magnetic parameters for the series of such complexes are presented in Table 1. According to the above qualitative analysis and formula (10), antiferromagnetism weakens sharply for these complexes at $\rho \to 90°$ and $\eta$ (N—N—Ni angle) $\to 180°$. The experimental data were quantitatively interpreted by the theoretical expression written for the $\sigma$-orbitals of the $Ni^{II}$ atoms

$$-2J = Af1[-\sin\eta_1\sin\eta_2\cos\rho + x1|x1|\cos\eta_1\cos\eta_2]^2 + Fe1, \qquad (11)$$

where Fe1 is the ferromagnetic contribution. The interactions of the $\sigma$-orbitals ($d_{xy}$) of the $Ni^{II}$ atoms with the $|y,z-\rangle$ orbitals (see formula (10)) and the term caused by the incomplete compensation of contributions from the $|x\pm\rangle$ orbitals are taken into account in the antiferromagnetic contribution. In addition to the experimental $-2J_{exp}$ values, the theoretical estimations of $-2J_{th}$ obtained by formula (11) and the corresponding parameters of the best approximation are presented in Table 1: Af1 = 161 cm$^{-1}$, $x1 = 0.45$, and Fe1 = $-14.4$ cm$^{-1}$. Since the $x1$ parameter is relatively low ($|x1|^2 \ll 1$), one can conclude that either the contributions of the $|x\pm\rangle$ orbitals are really compensated, or these contributions are low. However, in any case, it follows from the condition $x1 > 0$ that the $|x+\rangle$ contribution is higher than the $|x-\rangle$ contribution. Finally, the value $4S_aS_bAf1 \approx 600$ cm$^{-1}$ is close to the estimation of the maximum value of the antiferromagnetic exchange parameter in similar $Cu^{II}$ complexes. According to formula (2), this implies that for the $Ni^{II}$ compounds considered, the predominant contribution to antiferromagnetism is also caused by the $d_{xy}{}^a\text{—}N_3\text{—}d_{xy}{}^b$ interactions.

The main distinction of the $Ni(\mu_{1,3}\text{-}N_3)_2Ni$ complexes from the above-considered complexes is the doubled number of bridges. As follows from formulas (1) and (3) and the corresponding comments, $\Delta(ia,ib)$ and $-2J^f$ depend linearly on the number of bridges, and the dependence of $-2J^{af}$ is quadratic. Therefore, the experimental data in Table 2 were interpreted using the same formula (11); only redesignation Af1 $\to$ Af2 *etc.* was introduced for convenience. Unfortunately, the ($\eta_1$, $\eta_2$, $\rho$) sets in the two-bridge systems are much less representative for steric reasons than those in the one-bridge systems, so that the resulting parameters are strongly correlated. To decrease the corresponding uncertainty, the fixed value Af2 = 4Af1 = 644 cm$^{-1}$ was taken for the antiferromagnetic exchange parameter. The best approximation parameter

**Table 1.** Structural characteristics and exchange parameters $-2J$ ($cm^{-1}$) for the complexes containing the $[Ni(\mu_{1,3}\text{-}N_3)Ni]$ dinuclear fragments

| Complex[a] | N—N—Ni [b] | ρ | $-2J_{exp}$ ($-2J_{th}$)[c] | Ref. |
|---|---|---|---|---|
| | deg | | | |
| $[Ni(tmd)_2(\mu\text{-}N_3)]_n(ClO_4)_n$ (**1**) | 120.9, 120.9 | 180.0 | 100.0 (103.7) | 20 |
| $[Ni(macro)_2(\mu\text{-}N_3)]_n(ClO_4)_n$ (**2**) | 115.6, 116.8 | 175.7 | 97.8 (100.2) | 21 |
| $[Ni_2(333\text{-}tet)_2(\mu\text{-}N_3)]_n(ClO_4)_n$ (**3**)[d] | 123.6, 123.6 | 180.0 | 80.7 (78.0) | 22 |
| | 142.4, 142.4 | 180.0 | 37.4 (26.0) | |
| $[Ni(tmd)_2(\mu\text{-}N_3)]_n(PF_6)_n$ (**4**) | 126.1, 126.1 | 180.0 | 70.6 (70.2) | 23 |
| $[Ni(323\text{-}tet)_2(\mu\text{-}N_3)]_n(ClO_4)_n$ (**5**) | 135.8, 119.8 | 169.3 | 62.7 (57.5) | 24 |
| $[Ni_2(trenpy)_2(\mu\text{-}N_3)](ClO_4)_3$ (**6**) | 131.6, 131.6 | 180.0 | 53.6 (53.7) | 25 |
| $[Ni(cth)_2(\mu\text{-}N_3)]_n(ClO_4)_n$ (**7**)[e] | 128.5, 130.7 | 150.5 | 41.1 (42.6) | 26 |
| | 131.4, 131.4 | 146.2 | 36.4 (35.7) | |
| $[Ni(2,2'\text{-}mettn)_2(\mu\text{-}N_3)]_n(PF_6)_n$ (**8**) | 136.5, 136.5 | 180.0 | 41.1 (40.2) | 23 |
| $[Ni_2(cyclam)_2(\mu\text{-}N_3)]_n(ClO_4)_n$ (**9**) | 140.7, 128.2 | 166.9 | 39.2 (40.4) | 27 |
| $[Ni(bipy)_2(\mu\text{-}N_3)]_n(ClO_4)_n$ (**10**) | 125.0, 120.7 | 135.5 | 33.0 (36.4) | 28 |
| $[Ni_2(232\text{-}tet)_2(\mu\text{-}N_3)]_n(ClO_4)_n$ (**11**) | 134.6, 124.1 | 142.4 | 26.9 (36.0) | 24 |
| $[Ni_2(Me_4cyclam)_2(N_3)_2(\mu\text{-}N_3)]I$ (**12**) | 142.0, 142.0 | 180.0 | 24.6 (24.9) | 29, 30 |
| $[Ni(2\text{-}methyl)_2(\mu\text{-}N_3)]_n(ClO_4)$ (**13**) | 131.8, 125.9 | 125.9 | 16.8 (16.0) | 31 |
| $[Ni_2(L)(H_2O)(\mu\text{-}N_3)](CF_3SO_3)_2$ (**14**) | 165.8, 157.6 | 0.00 | −11.8 (−13.1) | 12 |

[a] Designations: tdm is 1,3-diaminopropane, macro is 2,3-dimethyl-1,4,8,11-tetraazacyclotetradeca-1,3-diene; trenpy is *N*,*N*-bis(2-aminoethyl)-*N*′-2-(pyridylmethyl)ethane-1,2-diamine; $Me_4$cyclam is 1,4,8,11-tetramethyl-1,4,8,11-tetraazacyclotetradecane; 2,2′-mettn is 2,2′-dimethyl-1,3-diaminopropane; 232-tet is *N*,*N*′-bis(2-aminoethyl)-1,3-diaminopropane; 323-tet is *N*,*N*′-bis(2-aminopropyl)-1,3-diaminopropane; 333-tet is *N*,*N*′-bis(3-aminopropyl)-1,3-diaminopropane; cth is *meso*-5,7,7,12,14,14-hexamethyl-1,4,8,11-tetraazacyclotetradecane; 2-methyl is 1,2-diamino-2-methylpropane.

[b] The pairwise values of angles are caused by the coordination of the NNN ligands.

[c] The $2J_{th}$ values were obtained by formula (11) for Af1 = 161 $cm^{-1}$, $x1 = 0.45$, and Fe1 = −14.4 $cm^{-1}$.

[d] Alternated chain.

[e] Two structurally different chains.

$x2 = 0.34$ somewhat differs from $x1$, and Fe2 = −25 $cm^{-1}$ differs from 2Fe1. This is not surprising, because $x$ and Fe are, in essence, small corrections to Af. The theoretical $-2J$ values calculated with these parameters are close to the experimental values (see Table 2), although the consistence is somewhat worse than in the case of the one-

**Table 2.** Structural characteristics and exchange parameters $-2J$ ($cm^{-1}$) for the complexes containing the $[Ni(\mu_{1,3}\text{-}N_3)_2Ni]$ dinuclear fragments

| Complex[a] | N—N—Ni [b] | ρ | $-2J_{exp}$ ($-2J_{th}$)[c] | Ref. |
|---|---|---|---|---|
| | deg | | | |
| $[Ni(N,N\text{-}dmen)(\mu\text{-}N_3)_2]_n$ (**21**) | 121.10, 139.40 | 0.0 | 156.0 (144.0) | 32, 33 |
| $[Ni(N,N'\text{-}dmen)(\mu\text{-}N_3)_2]_n$ (**22**) | 130.90, 134.90 | 0.0 | 120.0 (125.0) | 34 |
| $[Ni_2(1,3\text{-}pn)_4(\mu\text{-}N_3)_2](BPh_4)_2$ (**23**) | 127.70, 139.00 | 5.7 | 114.5 (113.7) | 35 |
| $[Ni_2(D,L\text{-}cth)_2(\mu\text{-}N_3)_2](ClO_4)_2$ (**24**) | 139.60, 127.40 | 6.6 | 113.0 (110.6) | 36 |
| $[Ni_2(222\text{-}tet)_2(\mu\text{-}N_3)_2](BPh_4)_2$ (**25**) | 128.50, 129.90 | 41.7 | 83.6 (79.5) | 37 |
| $[Ni(bpa)(\mu\text{-}N_3)_2]_n$ (**26**) | 136.50, 121.30 | 44.0 | 80.0 (68.0) | 38 |
| $[Ni_2(D,L\text{-}cth)_2(\mu\text{-}N_3)_2](PF_6)_2$ (**27**) | 124.30, 142.20 | 22.5 | 75.1 (86.2) | 36 |
| $[Ni_2(tren)_2(\mu\text{-}N_3)_2](BP_4)_2$ (**28**) | 123.30, 135.70 | 39.0 | 70.0 (81.3) | 30 |
| $[Ni_2(aep)_4(\mu\text{-}N_3)_2](PF_6)_2$ (**29**) | 126.70, 123.80 | 59.1 | 29.1 (32.0) | 39 |
| $[Ni_2(en)_4(\mu\text{-}N_3)_2](PF_6)_2$ (**30**) | 121.10, 119.30 | 70.5 | 4.6 (6.3) | 35 |

[a] Designations: 1,3-pn is 1,3-diaminopropane; tren is 2,2′,2″-triaminotriethylamine; aep is aminoethylpyridine; 222-tet is triethylenetetramine; cth is 5,5,7,12,12,14-hexamethyltetraazacyclotetradecane; dmen is dimethylethylenediamine; bpa is 1,2-bis(4-pyridyl)ethane.

[b] See footnote[b] in Table 1.

[c] The $-2J_{th}$ values were obtained by formula (11) for Af2 = 644 $cm^{-1}$, $x2 = 0.34$, and Fe2 = −25.0 $cm^{-1}$.

**Table 3.** Structural characteristics and exchange parameters $-2J$ ($cm^{-1}$) for the complexes containing the $[Mn(\mu_{1,3}\text{-}N_3)_2Mn]$ dinuclear fragments

| Complex | N—N—Ni [a] | ρ | $-2J_{exp}$ $(-2J_{th})$ [b] | Ref. |
|---|---|---|---|---|
| | deg | | | |
| $[Mn(3\text{-}Etpy)_2(\mu_{1,3}\text{-}N_3)_2]_n$ (**31**) [c] | 134.70, 131.70 | 13.5 | 11.7 (14.8) | 40 |
| | 134.80, 129.70 | 23.2 | 13.2 (13.9) | |
| $[Mn(bipy)_2(\mu_{1,3}\text{-}N_3)_2]_n$ (**32**) | 131.10, 127.30 | 41.1 | 11.9 (10.7) | 41 |
| $[Mn(pyOH)_2(\mu_{1,3}\text{-}N_3)_2]_n$ (**33**) | 123.80, 122.40 | 63.1 | 7.0 (3.1) | 40 |
| $[Mn(bpa)_2(\mu_{1,3}\text{-}N_3)_2]_n$ (**34**) [d] | 136.50, 121.30 | 44.0 | 5.7 (8.6) | 38 |

[a] See footnote [b] in Table 1.
[b] The $-2J_{th}$ values were obtained by formula (11) for Af3 = 100 $cm^{-1}$, $x3 = 0.45$, and Fe3 = $-4$ $cm^{-1}$.
[c] Alternated chain.
[d] bpa is 1,2-bis(4-pyridyl)ethane.

bridge systems. This is caused, most likely, by the influence of ignored distortions of the coordination polyhedra from the idealized tetragonal structure. These distortions are stronger in the two-bridge systems due to steric factors.

As can be seen from the data in Table 3, similar $Mn^{II}$ compounds also exhibit a distinct correlation of the $-2J_{exp}$ values to the η and ρ values. In this case, the theoretical $-2J_{th}$ values were obtained by formula (11) for the fixed values $x3 = x1 = 0.45$, Af3 = (4/25)Af2 ≈ 100 $cm^{-1}$, and Fe3 = (4/25)Fe2 ≈ $-4$ $cm^{-1}$. The estimates of two latter parameters are based on formula (2) under assumption that the predominant contribution to the antiferromagnetic exchange in the $Mn^{II}$ complexes is also caused by the $d_{xy}{}^a$—$N_3$—$d_{xy}{}^b$ overlaps. Here the agreement between the theory and experiment is much worse than that for the $Ni^{II}$ compounds. This should be expected, because other, ignored contributions in $-2J = \Sigma_{ij} - 2J_{ij}/(4S_aS_b)$ are added to the predominant contribution, which is described by formula (11). Each of the addition contributions is low but their number reaches 24, because the $Mn^{II}$ atoms have spins $S = 5/2$.

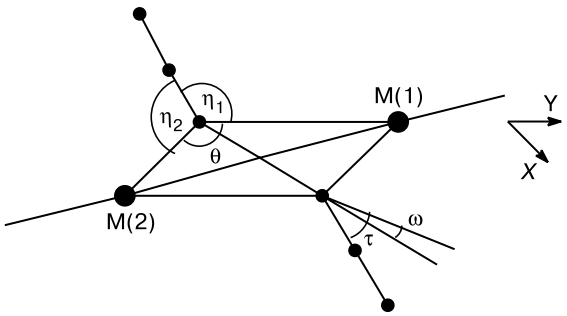


**Fig. 5.** Structures of the dinuclear fragments of the complexes with the $\mu_{1,1}$-$N_3$ bridging ligands; τ is the angle between $N_3$ and its projection to the M(1)—M(2)—N—N plane; ω is the angle between this projection and the bisectrix of the θ angle (N—M—N angle).

### Complexes with the $M(\mu_{1,1}\text{-}N_3)_2M$ magnetic fragments

Typical structures of these complexes are presented in Fig. 5. The M—N($N_3$)—M angles are designated by symbol θ; τ are the angles of shifts of the $N_3$ linear ligands from the M—N($N_3$)—M planes; the ω angles characterize the degree of asymmetry of arrangement of these ligands relatively to the bisectrix of the θ angles. The η angle (N—N—Ni angle) is usually presented in structural works instead of τ and ω. However, the τ and ω angles are more convenient for subsequent analysis.

Before considering experimental data, let us consider the formula for the one-ligand contribution to the Δ parameter corresponding to Fig. 5:

$$\Delta(\theta, \tau, \omega) \approx \sin^2\theta\{0.5[\cos\theta - \cos(2\omega)] + \quad (12a)$$

$$+ 0.5\sin^2\tau[\cos\theta + \cos(2\omega)] + \quad (12b)$$

$$+ 0.5c^2\cos^2\tau[\cos\theta + \cos(2\omega)] + 2cs\cos\tau\cos(\theta/2)\cos\omega + s^2\}. \quad (12c)$$

Here the common factor $\sin^2\theta$ is caused by the fact that for $\theta \neq 90°$ the orbitals of unpaired electrons $d_{xy}$ are not oriented exactly toward the ligand. The first term in brackets, which describes the effect of overlap with the $|y->$ orbital (see Figs. 3 and 5), does not need special comments, because it coincides (with an accuracy to $\omega \neq 0$) with the second term in Eq. (8). The amplitude factor $1/\sqrt{2}$, which is present in $|y->$, enters the constant. Formula (12b) describes the contribution of the $|z->$ orbital: its projection to the *xy* plane makes ~sinτ. As for the rest, the effect of $|z->$ is similar (with an accuracy to $\omega \neq 0$) to the effect of the $p_x$ orbital shown in Fig. 2, *b*.

It is somewhat more difficult to derive expressions for contributions of the $|x\pm>$ orbitals. Let us take into account that the orbitals of terminal atoms in the MO $|x\pm>$ are a linear combination of the $p_{x1}$ and $s_1$ functions (latter are not shown in Fig. 3). Then, for each of these MO, the

first and third matrices in formula (3) take the form $\alpha(p_{x1})\cos\tau\cos(\theta/2\pm\omega) + \alpha(s_1)$, and the whole expression (3) takes the form of formula (12c). Rigidly speaking, each MO $|x+>$ and $|x->$ has its set of the $c$ and $s$ coefficients. However, to avoid the appearance of a great number of unknown parameters, only one set is retained in formula (12). This seems to be not a very rough approximation, because two sets can be reduced to one set in realistic particular cases, when the contribution of one orbital predominates or both contributions are close.

For $c = 0$ and $s = 0$, expression (12) is transformed into the formula

$$\Delta \approx \sin^2\theta\{[\cos\theta - \cos(2\omega)] + \sin^2\tau[\cos\theta + \cos(2\omega)]\}/4, \quad (13)$$

which predicts a high $\Delta$ value and strong antiferromagnetism for any $\theta$, if $\tau \approx 0$ and $\omega \approx 0$. This situation, when $|c| \ll 1$, takes place in the complexes with the OR bridges[2,18,19] mentioned above.

In another limiting case when $c = 1$, formula (12) is transformed into expression (9), *i.e.*,

$$\Delta \approx \cos\theta + s^2. \quad (14)$$

Therefore, one should expect ferromagnetism or weak antiferromagnetism for $\theta \geq 90°$.

Now one can analyze the parameters for the $\mu_{1,1}$-$Cu^{II}$ complexes presented in Table 4.

It is seen that none of formulas (13) and (14) agrees with the experimental data. In fact, all complexes of this type are ferromagnetic. Thus, unlike the OR ligands, in the case of the $N_3$ symmetric ligands, the $|x>$ orbitals ($c \approx 0$) are not cancelled. At the same time, when the angle $\varepsilon = \theta - 90°$ increases in the complexes considered, an increase in the ferromagnetism slows down, *i.e.*, increasing the $-2J^{af}$ antiferromagnetic contribution, decreases. However, formula (14) predicts a linear increase in $\Delta$ and, hence, a quadratic increase in $-2J^{af}$. Thus, it should be expected that in the $\mu_{1,1}$-$Cu^{II}$ complexes $0 < |c| < 1$.

To obtain quantitative estimates, the experimental data were interpreted using the theoretical expression, which follows from formulas (1) and (12)

$$-2J_{th} = Af4[\Delta(\theta_1, \tau_1, \omega_1) + \Delta(\theta_2, \tau_2, \omega_2)]^2 + Fe4. \quad (15)$$

Although the coordination modes are different, the Af4 parameter in formula (15) has the same physical sense as Af1 for the $Ni^{II}$ complexes considered: for $\theta = 180°$ both of them describe the antiferromagnetic exchange through the $|y->$ orbital. Therefore, we can believe that $Af4 = 4S_aS_bAf1 = 644$ cm$^{-1}$. The other parameters obtained by the method of the best approximation of the $-2J_{th}$ values to $-2J_{exp}$ are the following: $c = 0.64$, $s = 0.171$, and $Fe4 = -290$ cm$^{-1}$. It is seen that the theory well describes the experiment, including the pronounced weakening of the ferromagnetic exchange in the series of compounds **41**—**44**, which is caused by the combined effect of simultaneous increasing $\theta$ and decreasing $\tau$. The relatively low value of the $c$ parameter should be treated carefully. First, the $c$ and $s$ values are strongly correlated due to the low representation of experimental data. Second, the error in $-2J_{exp}$ for strongly ferromagnetic compounds can be considerable, because for $-2J < -50$ cm$^{-1}$ the change in the effective magnetic moment is only 10—15% in the whole temperature interval. For instance, for compound **45**, $-2J_{exp} = -70\pm20$ cm$^{-1}$.[16] Therefore, the $c$ value can be much higher and $s$ can be lower. Weakening of the $-2J_{th}(\theta)$ function with approaching $c$ to 1 results in a greater discrepancy between the theory and experiment; however, the error of the theory does not exceed the experimental error down to $c \approx 0.9$.

From the viewpoint of the ferromagnetism theory, it is of great interest why $|Fe4|$ is much higher than $4S_aS_b|Fe2| \approx 100$ cm$^{-1}$? This effect can be explained as follows.

According to the generalized angular overlap model,[3,4] the columns of the first matrix in formula (3) are the admixing coefficients of ligands to the total wave functions. This implies that the antibonding MO of the

**Table 4.** Structural characteristics and exchange parameters $-2J$ (cm$^{-1}$) for the complexes containing the $[Cu(\mu_{1,1}\text{-}N_3)_2Cu]$ dinuclear fragments

| Complex[a] | θ | τ | ω | $-2J_{exp}$ ($-2J_{th}$) | Ref. |
|---|---|---|---|---|---|
| | deg | | | | |
| $[Cu_2(\mu_{1,1}\text{-}N_3)_2(3\text{-ampy})_4(\mu\text{-}NO_3)_2]\cdot EtOH$ (**41**) | 97.5, 97.5 | 36.2, 35.6 | 1.6, 2.0 | −223.0 (−223) | 42 |
| $[Cu_2(\mu_{1,1}\text{-}N_3)_2(4\text{-Etpy})_4(\mu\text{-}NO_3)_2]$ (**42**) | 98.2, 98.2 | 32.0, 32.0 | 1.6, 1.6 | −230.0 (−205) | 42 |
| $[Cu_2(\mu_{1,1}\text{-}N_3)_2(dmptd)(N_3)_2]$ (**43**) | 98.0, 101.4 | 38.1, 22.8 | 1.0, 0.3 | −170.0 (−179) | 43 |
| $[Cu_2(\mu_{1,1}\text{-}N_3)_2(Bu^tpy)_4](ClO_4)$ (**44**) | 100.5, 100.5 | 4.5, 4.5 | 4.8, 4.8 | −105.0 (−120) | 44 |
| $[Cu_2(\mu_{1,1}\text{-}N_3)_2[24]ane\text{-}N_2O_6](H_2O)$ (**45**) | 105.5, 101.6 | 8.8, 4.9 | 1.9, 2.7 | −70.0 (−61) | 16 |
| $[Cu_2(tbz)(\mu_{1,1}\text{-}N_3)_2](MeOH)_2$ (**46**) | 104.5, 104.5 | 4.7, 4.7 | 3.0, 3.0 | −46.0 (−41) | 45 |

[a] Designations: 3-ampy is 3-aminopyridine; 4-Etpy is 4-ethylpyridine; dmptd is 2,5-bis((pyridinemethyl)thio)thiadiazole; [24]ane-$N_2O_6$ is polyaza-polyoxomacrocyclic ligand; $HL^2$ is 1-(2-hydroxybenzyl)-1,5-diazacyclooctane; tbz is bis(2-benzimidazolyl)propane.
[b] The $-2J_{th}$ values were obtained by formula (15) for $Af4 = 644$ cm$^{-1}$, $c = 0.64$, $s = 0.17$, and $Fe4 = -290$ cm$^{-1}$.

**Table 5.** Structural characteristics and exchange parameters $-2J$ ($cm^{-1}$) for the complexes containing $[Ni(\mu_{1,1}\text{-}N_3)_2Ni]$ dinuclear fragments

| Complex* | θ | τ | ω | $-2J_{exp}$ | Ref. |
|---|---|---|---|---|---|
| | deg | | | | |
| $[Ni_2(\mu_{1,1}\text{-}N_3)_2(terpy)_2(N_3)_2]\cdot 2H_2O$ (**51**) | 101.3, 101.3 | 0.0, 0.0 | 0.0, 0.0 | −40.2 | 46 |
| $[Ni(\mu_{1,1}\text{-}N_3)(N_3)(terpy)(N_3)]_2\cdot H_2O$ (**52**) | 101.6, 101.6 | 13.8, 13.8 | 3.3, 3.3 | −45.6 | 47 |
| $[Ni_2(\mu_{1,1}\text{-}N_3)_2(Me_3[12]N_3)_2](ClO_4)_2$ (**53**) | 103.8, 103.8 | 18.9, 18.9 | 5.0, 5.0 | −43.9 | 48 |
| $[Ni_2(\mu_{1,1}\text{-}N_3)_2(N_3)_2(Medpt)_2]$ (**54**) | 104.0, 104.0 | 0.0, 0.0 | 5.5, 5.5 | −46.7 | 49, 50 |
| $[Ni_2(\mu_{1,1}\text{-}N_3)_2(en)_4](ClO_4)_2$ (**55**) | 104.3, 104.3 | 4.7, 4.7 | 5.9, 5.9 | −43.4 | 51 |
| $[Ni_2(\mu_{1,1}\text{-}N_3)_2(232\text{-tet})_2](PF_6)_2$ (**56**) | 104.6, 104.6 | 0.0, 0.0 | 4.2, 4.2 | −34.3 | 52 |
| $[Ni_2(\mu_{1,1}\text{-}N_3)_2(232\text{-}N_4)_2](ClO_4)_2$ (**57**) | 104.9, 104.9 | 0.0, 0.0 | 0.0, 0.0 | −33.8 | 48 |
| $[Ni_2(\mu_{1,1}\text{-}N_3)_2(terpy)_2(N_3)(H_2O)]ClO_4$ (**58**) | 102.4, 100.6 | 23.1, 26.0 | 4.6, 5.2 | −27.2 | 47 |
| $[Ni_2(\mu_{1,1}\text{-}N_3)_2(pepci)_2(N_3)_2)]\cdot 2H_2O$ (**59**) | 102.2, 101.0 | 27.6, 14.6 | 0.0, 0.0 | −72.6 | 53 |

* Designations: terpy is 2,2′:6′,6″-terpyridine; $Me_3[12]N_3$ is 2,4,4-trimethyl-1,5,9-triazacyclodec-1-ene; 232-$N_4$ is *N*,*N*′-bis(2-aminoethyl)-1,3-diaminopropane; Medpt is methyl-bis(3-aminopropylamine); 232-tet is *N*,*N*′-bis(2-aminoethyl)-1,3-diaminopropane; pepci is *N*′-(2-ethyl-2-pyridine)pyridine-2-carbamide.

$\mu_{1,3}$-complexes appear as $|\psi> \sim |a> \pm |b> + |y->$. The $|y->$ orbital is strongly delocalized (see Fig. 3), so that the interelectron repulsion and the related ferromagnetic interaction are low. At the same time, for the $\mu_{1,1}$-complexes, $|\psi+> \sim |a> + |b> + |x+> + |x->$. As can be seen from the data in Fig. 3, the combination $|x+> + |x-> \sim \alpha p_{x1} + \beta s_1$ is localized on the coordinated atoms of the ligand, unlike its MO. This can result in a sharp increase in the ferromagnetic contribution on going from the $\mu_{1,3}$ coordination mode to $\mu_{1,1}$. In addition, a considerable contribution caused by spin polarization[5] can appear in the $\mu_{1,1}$-complexes, because the published data[6] do not completely exclude the presence of this contribution.

In conclusion, let us consider the $L_nNi(\mu_{1,1}\text{-}N_3)_2NiL_n$ complexes. As can be seen from the data in Table 5, for compounds **51**—**57** with a very representative set of angle values θ = 101—105° and τ = 0—20°, the experimental values of exchange parameters are within a narrow interval (−40±5 $cm^{-1}$). At the same time, compounds **58** and **59** have rather close structural parameters, although the values $-2J_{exp} = -27.2$ and $-72.6$ $cm^{-1}$ differ very strongly. It is very probable that such paradoxical results can be explained by difficulties in interpretation of experimental data for ferromagnetic compounds. In the case of the $Ni^{II}$ complexes, these difficulties are aggravated by the strong splitting in the zero field, whose parameter *D* is strongly correlated to $-2J$. It is most likely that the $Ni^{II}$ complexes require additional studies using, perhaps, thermodynamic and spectroscopic methods. Despite possible errors, it seems doubtless that the $\mu_{1,1}$-$Ni^{II}$ complexes are characterized by high negative $D \approx -10$——$-20$ $cm^{-1}$.[46—53] Since such *D* values are a necessary condition for the effect of magnetic memory,[54] additional studies of the $\mu_{1,1}$-$Ni^{II}$ complexes are urgent from the viewpoint of the general problem of molecular magnetic design.

This work was financially supported by the Russian Foundation for Basic Research (Project No. 03-03-32517).

## References

1. O. Kahn, *Molecular Magnetism*, VCH Publishers, Inc., 1993, 373 pp.
2. Yu. V. Rakitin and V. T. Kalinnikov, *Sovremennaya magnetokhimiya* [*Modern Magnetochemistry*], Nauka, St. Petersburg, 1994, 272 pp. (in Russian).
3. Yu. V. Rakitin, S. G. Khodasevich, and V. T. Kalinnikov, *Koord. Khim.*, 1997, **23**, 3; 13 [*Russ. J. Coord. Chem.*, 1997, **23**, No. 1 (Engl. Transl.)].
4. Yu. V. Rakitin and V. T. Kalinnikov, *Model´ uglovogo perekryvaniya v teorii stroeniya soedinenii perekhodnykh metallov* [*The Model of Angular Overlap in the Theory of Structure of Transition Metals*], Izd-vo KNTs RAN, Apatity, 2000, 306 pp. (in Russian).
5. M.-F. Charlot, O. Kahn, M. Chaillet, and Ch. Larieu, *J. Am. Chem. Soc.*, 1986, **108**, 2574.
6. M. A. Aebersold, B. Gillon, O. Plantevin, and L. Pardi, O. Kahn, P. Bergarat, I. von Seggern, F. Tuczek, L. Ohrstron, A. Grand, and E. Leviever-Berna, *J. Am. Chem. Soc.*, 1998, **120**, 5238.
7. P. J. Hay, J. C. Thibeault, and R. Hoffman, *J. Am. Chem. Soc.*, 1975, **97**, 4884.
8. Yu. V. Rakitin, A. E. Vetrov, and V. T. Kalinnikov, *Koord. Khim.*, 1995, **21**, 680 [*Russ. J. Coord. Chem.*, 1995, **21**, No. 9 (Engl. Transl.)].
9. P. W. Anderson, *Exchange in Insulators: Superexchange, Direct Exchange, and Double Exchange. Magnetism*, Eds. G. T. Rado and H. Suhl, Acad. Press, New York, 1963, **1**, 25.
10. R. S. Mulliken, *J. Chim. Phys.*, 1949, **46**, 497.
11. M. Wolfsberg and L. Helmholz, *J. Chem. Phys.*, 1952, **20**, 837.
12. A. Escuer, C. J. Harding, Y. Dussart, J. Nelson, V. McKee, and R. Vicente, *J. Chem. Soc., Dalton Trans.*, 1999, 223.

13. I. Bkouche-Wasman, M.-L. Boillot, O. Kahn, and S. Sikorav, *Inorg. Chem.*, 1984, **23**, 4454.
14. Ph. Chudhuri, K. Oder, K. Wieghardt, B. Nuber, and J. Weiss, *Inorg. Chem.*, 1986, **25**, 2818.
15. Y. Agnus, R. Louis, and R. Weiss, *J. Am. Chem. Soc.*, 1979, **101**, 3381.
16. J. Comatmond, P. Plumere, J.-M. Lehn, Y. Agnus, R. Loius, R. Weiss, and O. Kahn, *J. Am. Chem. Soc.*, 1982, **104**, 6330.
17. F. Tuczek and W. Bensch, *Inorg. Chem.*, 1995, **34**, 1486.
18. Yu. V. Rakitin and V. V. Volkov, *Koord. Khim.*, 1986, **12**, 1509 [*Sov. J. Coord. Chem.*, 1986, **12**, No. 11 (Engl. Transl.)].
19. *Molecule-Based Magnetic Materials*, Eds. M. M. Turnbull, T. Sugimoto, and L. K. Thompson, ACS Symposium Ser., 1995, **644**, Ch. 11, 170.
20. X. Solans, C. Diaz, M. Monfort, and J. Ribas, *XV Intern. Crystallogr. Meeting*, Burdeos, 1990, 154.
21. A. Escuer, R. Vicente, J. Ribas, M. S. El Fallah, X. Solans, and M. Font-Bardia, *Inorg. Chem.*, 1995, **34**, 1278.
22. A. Escuer, R. Vicente, J. Ribas, M. S. El Fallah, X. Solans, and M. Font-Bardia, *Inorg. Chem.*, 1994, **33**, 1842.
23. M. Monfort, J. Ribas, X. Solans, and M. Font-Bardia, *Inorg. Chem.*, 1996, **35**, 7633.
24. A. Escuer, R. Vicente, J. Ribas, M. S. El Fallah, X. Solans, and M. Font-Bardia, *Inorg. Chem.*, 1993, **32**, 3727.
25. G. A. McLachlan, C. D. Fallon, R. L. Martin, B. Moubaraki, K. S. Murray, and L. Spiccia, *Inorg. Chem.*, 1994, **33**, 4663.
26. A. Escuer, R. Vicente, J. Ribas, M. S. El Fallah, X. Solans, and M. Font-Bardia, *J. Chem. Soc.*, *Dalton Trans.*, 1993, 2975.
27. A. Escuer, R. Vicente, J. Ribas, M. S. El Fallah, and X. Solans, *Inorg. Chem.*, 1993, **32**, 1033.
28. R. Cortes, K. Urtiaga, L. Lezama, J. L. Pizarro, A. Goni, M. I. Arriortua, and T. Rojo, *Inorg. Chem.*, 1994, **33**, 4009.
29. F. Wagner, M. T. Mocella, M. J. D´Aniello, A. H.-J. Wang, and E. K. Barefield, *J. Am. Chem. Soc.*, 1974, **96**, 2625.
30. C. G. Pierpont, D. N. Hendrickson, D. M. Duggan, F. Wagner, and E. K. Barefield, *Inorg. Chem.*, 1975, **14**, 604.
31. J. Ribas, M. Monford, C. Diaz, C. Bastos, C. Mer, and X. Solans, *Inorg. Chem.*, 1995, **34**, 4986.
32. J. Ribas, M. Monfort, B. Kumar-Gosh, X. Solans, and M. Font-Bardia, *J. Chem. Soc.*, *Chem. Commun.*, 1995, 2375.
33. A. Esposito, G. Kamieniarz, *Phys. Rev.*, 1998, **B57**, 7431.
34. J. Ribas, M. Monfort, I. Resino, X. Solans, P. Rabu, F. Maingot, and M. Drillon, *Angew. Chem.*, *Int. Ed. Engl.*, 1996, **35**, 2520.
35. J. Ribas, M. Monford, C. Diaz, C. Bastos, and X. Solans, *Inorg. Chem.*, 1993, **32**, 3557.
36. A. Escuer, R. Vicente, M. S. El Fallah, X. Solans, and M. Font-Bardia, *Inorg. Chim. Acta*, 1998, **278**, 43.
37. A. Escuer, I. Castro, F. A. Mautner, M. S. El Fallah, and R. Vicente, *Inorg. Chem.*, 1997, **36**, 4633.
38. M. L. Hernandes, M. G. Barandika, M. K. Urtiaga, R. Cortes, L. Lezama, and M. I. Arriotua, *J. Chem. Soc.*, *Dalton Trans.*, 2000, 79.
39. J. Ribas, M. Monfort, B. Kumar-Gosh, R. Cortes, X. Solans, and M. Font-Bardia, *Inorg. Chem.*, 1996, **35**, 864.
40. A. Escuer, R. Vicente, M. A. S. Goher, F. A. Mautner, *Inorg. Chem.*, 1998, **37**, 782.
41. G. Viau, M. G. Lombardi, G. De Munno, M. Julve, F. Lloret, J. Faus, A. Caneschi, and J. M. Clemente-Juan, *Chem. Commun.*, 1997, 1195.
42. A. Escuer, M. A. S. Goher, F. A. Mautner, and R. Vicinte, *Inorg. Chem.*, 2000, **39**, 2107.
43. S. S. Tandon, L. K. Thompson, M. E. Manuel, and J. N. Bridson, *Inorg. Chem.*, 1994, **33**, 5555.
44. S. Sikorav, I. Bkouche-Wasman, and O. Kahn, *Inorg. Chem.*, 1984, **23**, 490.
45. G. A. van Albada, M. T. Lakin, N. Veldman, A. L. Spek, and J. Reedijk, *Inorg. Chem.*, 1995, **34**, 4910.
46. M. I. Arriortua, R. Cortes, K. Urtiaga, L. Lezama, T. Rojo, X. Solans, and M. Font-Bardia, *Inorg. Chim. Acta*, 1990, 263.
47. M. G. Barandika, R. Cortes, L. Lezama, M. K. Urtiaga, M. I. Arriortua, and T. Rojo, *J. Chem. Soc.*, *Dalton Trans.*, 1999, 2971.
48. R. Vicente, A. Escuer, J. Ribas, M. S. El Fallah, X. Solans, and M. Font-Bardia, *Inorg. Chem.*, 1993, **32**, 1920.
49. A. Escuer, R. Vicente, J. Ribas, and X. Solans, *Inorg. Chem.*, 1995, **34**, 1793.
50. A. Escuer, R. Vicente, J. Ribas, and X. Solans, *J. Magn. Magn. Mat.*, 1992, **110**, 181.
51. J. Ribas, M. Monfort, C. Diaz, C. Bastos, and X. M. Solans, *Inorg. Chem.*, 1994, **33**, 484.
52. A. Escuer, R. Vicente, M. S. El Fallah, X. Solans, and M. Font-Bardia, *Inorg. Chim. Acta.*, 1996, **247**, 85.
53. R. Cortes, J. I. R. Larramendi, L. Lezama, T. Rojo, K. Urtiaga, and M. I. Arriortua, *J. Chem. Soc.*, *Dalton Trans.*, 1992, 2723.
54. V. M. Novotortsev, V. T. Kalinnikov, and Yu. V. Rakitin, *Usp. Khim.*, 2003, **72**, 1123 [*Russ. Chem. Rev.*, 2003, **72**, No. 12 (Engl. Transl.)].

*Received November 12, 2003*